Heliyon 11 (2025) e40104

Contents lists available at ScienceDirect

Heliyon

journal homepage: www.cell.com/heliyon

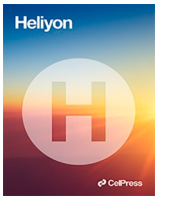

Research article

Eco-friendly synthesis of gold nanoparticles via *tangerine* peel extract: Unveiling their multifaceted biological and catalytic potentials

Seyedeh Masoumeh Ghoreishi [a], Sobhan Mortazavi-Derazkola [b,c,*]

[a] *Cellular and Molecular Biology Research Center, Health Research Institute, Babol University of Medical Sciences, Babol, Iran*
[b] *Medical Toxicology and Drug Abuse Research Center (MTDRC), Birjand University of Medical Sciences, Birjand, Iran*
[c] *School of Chemistry and Astbury Centre for Structural Molecular Biology, University of Leeds, Leeds, LS2 9JT, United Kingdom*

ARTICLE INFO

Keywords:
Gold nanoparticles
Green synthesis
Antibacterial
Photocatalyst

ABSTRACT

Recent advancements in nanoscience underscore the transformative potential of nanomaterials in environmental and biological applications. In this study, we synthesized gold nanoparticles (Au@*TPE* NPs) using an eco-friendly and cost-effective approach, leveraging *tangerine* peel extract as both a capping and reducing agent. This method presents a sustainable alternative to traditional chemical agents. We optimized synthesis parameters, including time (5, 30, 60, and 90 min), temperature (25, 40, and 60 °C), and gold concentration (5, 10, 15, and 20 mM) to refine the nanoparticles size and morphology. Characterization via UV–Vis, XRD, FT-IR, EDAX, FESEM, and TEM revealed that nanoparticles synthesized at 40 °C and 15 mM gold concentration exhibited an optimal size (~26 ± 5 nm) and a spherical shape. The Au@*TPE* NPs demonstrated antibacterial activity against both Gram-positive and Gram-negative bacteria, with minimum inhibitory concentrations (MIC) of 31.25 μg/ml for *Klebsiella pneumoniae* and *Escherichia coli*, and 62.5 μg/ml for *Pseudomonas aeruginosa*. Notably, they also exhibited antifungal activity against *Candida albicans* and demonstrated 92.7 % antioxidant activity in a DPPH scavenging assay at 250 μg/ml. Photocatalytic tests revealed that the nanoparticles effectively degraded methyl orange and rhodamine B, achieving 88.6 % and 93.2 % degradation under UV light, respectively, and 67.3 % and 74.1 % degradation under sunlight. These promising biological and catalytic properties suggest significant potential for diverse applications.

1. Introduction

Nanotechnology, a field dedicated to the development and application of nanoparticles, has made significant strides across various scientific disciplines, revealing novel solutions to complex challenges. Nanoparticles are typically characterized by their dimensions, which range from 1 to 100 nm in at least one direction. In the medical field, this technology has led to the emergence of nanomedicine, which enhances our ability to diagnose, monitor, and treat diseases. By leveraging nanoparticles, nanotechnology addresses a wide array of pharmacological issues, providing innovative approaches to managing and treating diverse medical conditions [1–3]. Nanoparticles have been used in various fields such as medicine, pharmaceuticals, and engineering [4–6]. Various methods for synthesizing nanoparticles have been introduced, including hydrothermal, chemical vapor deposition, and sol-gel techniques [7–9]. Each

* Corresponding author. Medical Toxicology and Drug Abuse Research Center (MTDRC), Birjand University of Medical Sciences, Birjand, Iran.
E-mail address: S.mortazavi23@yahoo.com (S. Mortazavi-Derazkola).

https://doi.org/10.1016/j.heliyon.2024.e40104
Received 19 August 2024; Received in revised form 4 October 2024; Accepted 1 November 2024
Available online 7 November 2024

of these methods has its own set of advantages and disadvantages. However, a major drawback common to these approaches is their high cost and reliance on chemical reducing agents. Consequently, the development of a simpler and more cost-effective method that utilizes natural materials instead of chemical reducing agents would significantly benefit the environment. One such approach is the synthesis of nanoparticles using green chemistry methods.

The green synthesis of nanoparticles has become increasingly prominent in materials and nanoscience research, thanks to its numerous benefits. This method is particularly valued for its environmentally friendly approach, as it avoids the use of toxic substances and hazardous chemicals. Additionally, it adheres to high safety standards and results in minimal environmental impact, making it a sustainable and safer alternative to traditional nanoparticle synthesis techniques [10,11]. Green synthesis utilizing plants is increasingly favored due to their abundant bioactive phytochemicals, such as phenolics, alkaloids, steroids, curcumins, and flavonoids. These compounds, while chemically complex, are environmentally benign and can act as reducing, capping, and stabilizing agents in nanoparticle synthesis. Consequently, plant-based methods yield highly stable nanoparticles, which not only streamline the scaling-up process but also significantly reduce the risk of contamination [12,13]. In recent years, various extracts have been used for the synthesis of nanoparticles, such as *Solanum tuberosum* [14], *Capsicum annum* [15], *Zingiber officinale* [16,17], *barberry* [18], *Crataegus microphylla* [19].

Metal nanoparticles have significantly advanced the field of nanotechnology, offering promising applications across various domains. Their contributions are particularly noteworthy in nano-drug delivery, where they facilitate targeted and efficient medication transport; nano-biosensing, which enhances the sensitivity and accuracy of biological detection; and antibacterial and antifungal therapeutics, where they provide effective solutions for combating microbial infections. Additionally, these nanoparticles are instrumental in photocatalysis, where they drive chemical reactions under light exposure, leading to applications such as environmental remediation and energy conversion. These diverse functionalities underscore the transformative impact of metal nanoparticles on both scientific research and practical technologies [20–25].

Among metallic nanoparticles, gold nanoparticles (AuNPs) have a well-established history of medicinal use. They are renowned for their high stability, low reactivity, excellent biocompatibility, and minimal toxicity in biological systems. Additionally, AuNPs are characterized by a high surface-to-volume ratio and possess distinctive optical, electronic, scattering, and absorption properties. Their tunable surface plasmon resonance and facile surface functionalization have made them valuable in a variety of applications, including electronics, sensing, environmental monitoring, therapeutics, and biological fields [26]. Furthermore, AuNPs have been extensively studied for their diverse biological activities, such as antibacterial [27], anticancer [28], antifungal [29], antioxidant [30], and wound healing [31] effects. Deepti Susanna et al. reported a method for synthesizing gold nanoparticles (AuNPs) from *Nothapodytes foetida* leaves using ultrasonication. The AuNPs, characterized by UV absorption at 524 nm and various analytical techniques, were stable, mostly spherical, and ranged from 5 to 30 nm in size. The synthesized AuNPs showed strong antioxidant, antibacterial, and anticancer properties, and demonstrated significant wound-healing effects. These findings highlight the AuNPs for various applications [32]. Samson Rokkarukala et al. reported the green synthesis of gold nanoparticles (AuNPs) using *Sarcophyton crassocaule* marine coral extract. TEM and SEM revealed spherical and oval AuNPs ranging from 5 to 50 nm in size. The nanoparticles showed excellent stability, as confirmed by zeta potential and FT-IR analysis. The synthesized AuNPs demonstrated significant biological activities: strong antibacterial effects, high antioxidant capacity (DPPH: 85 %, RP: 82 %), and notable anti-diabetic activity (inhibition of α-amylase: 68 %, α-glucosidase: 79 %). They also exhibited 91 % catalytic effectiveness in reducing hazardous organic dyes [33]. Princy and colleagues investigated the synthesized gold and silver nanoparticles using *Solanum nigrum* root extract. The nanoparticles had diameters of 22.35 nm (gold) and 11.85 nm (silver) with 5 ml extract, and 16.06 nm (gold) and 8.72 nm (silver) with 10 ml extract. They showed strong antibacterial activity, especially against *Staphylococcus aureus*. In vitro tests revealed potential in treating lung cancer with A549 cells. The nanoparticles also excelled in photocatalytic degradation of methylene blue and methylene orange. The results highlight their potential for cancer therapy, antibacterial use, and environmental cleanup [34].

In this study, gold nanoparticles were synthesized using a green chemistry method in the presence of *tangerine* peel extract. After characterizing the synthesized nanoparticles, their anticancer, antioxidant, catalytic, and antibacterial activities against both Gram-positive and Gram-negative strains were evaluated. The results indicated that the synthesized nanoparticles exhibited significant antibacterial activity against Gram-negative strains, as well as high antioxidant and anticancer activities. Additionally, the degradation of rhodamine b and methyl orange in the presence of the synthesized gold nanoparticles demonstrated their potential as a suitable alternative for environmental applications.

2. Experimental

2.1. Materials

Gold (III) chloride trihydrate ($HAuCl_4.3H_2O$, 99.99 %), methyl orange (99 % pure), rhodamine B (99 % pure), methanol (HPLC gradient grade, 99.9 %), and ethanol were purchased from Sigma-Aldrich. Deionized (DI) water was utilized in all processes. The chemicals were used as received without further purification. *Klebsiella pneumoniae*, *Pseudomonas aeruginosa*, *Escherichia coli*, *Streptococcus mutans, Streptococcus salivarius*, and *Staphylococcus aureus* were obtained from the Pasteur Institute of Iran.

2.2. Extraction of tangerine peel (TPE)

The fresh tangerine peels were washed several times with water and finally rinsed with deionized distilled water to remove impurities. The peels were then cut into smaller pieces, air-dried, and subsequently dried in an oven at 40 °C for approximately 48 h. After

Table 1
Synthesis of gold nanoparticles using *tangerine* peel extract under various conditions such as temperature, time, and concentration.

Sample	Au concentration (mM)	Temperature (°C)	Time (min)	Figure of UV/Vis
1	5	40	60	Fig. 1a
2	10	40	60	Fig. 1a
3	15	40	60	Fig. 1a
4	20	40	60	Fig. 1a
5	15	25	60	Fig. 1b
6	15	60	60	Fig. 1b
7	15	40	5	Fig. 1c
8	15	40	30	Fig. 1c
9	15	40	90	Fig. 1c

drying, the peels were ground into a powder using a blender. Subsequently, 200 g of the dried *tangerine* peel powder was extracted with 250 ml of methanol on a shaker for 72 h. Following this period, the extract was filtered. The methanol solvent was then removed using a rotary evaporator. The final extract was stored in a refrigerator for the synthesis of gold nanoparticles.

2.3. Synthesis of gold nanoparticles using tangerine peel extract (Au@TPE NPs)

In this study, gold nanoparticles were synthesized using a green synthesis method adapted from the procedure described by Shirzadi-Ahodashti et al. [35] with slight modifications. Initially, 10 mM of gold salt was dissolved in 10 ml of distilled water under vigorous stirring. Subsequently, 10 ml of *TPE* extract were gently added to the reaction vessel at room temperature (25 °C). The reaction proceeded for 60 min, during which the color of the solution changed from pale yellow to deep red. This color change is attributed to a phenomenon known as surface plasmon resonance (SPR), indicating the formation of gold nanoparticles. Finally, the synthesized nanoparticles were collected by centrifugation for 20 min, followed by three washings. The nanoparticles were then dried at room temperature for 24 h. To achieve the optimal size and morphology of the nanoparticles, optimization of time, temperature, and concentration was performed (Table .1).

2.4. Antibacterial and antifungal activity

The antibacterial and antifungal activities of *tangerine* peel extract and gold nanoparticles synthesized with *TPE* extract (sample no. 9) were evaluated against strains of *Klebsiella pneumoniae*, *Pseudomonas aeruginosa*, *Escherichia coli*, *Streptococcus mutans, Streptococcus salivarius*, *Staphylococcus aureus*, and *Candida albicans*. The microdilution broth method was employed for the assessment. Different concentrations of nanoparticles and extract were prepared by adding 100 µl of Mueller-Hinton broth to a 96-well microplate. The tested concentrations for nanoparticles were 1000, 500, 250, 125, 62.5, 31.25, and 15.62 µg/ml, while for the extract, they were 4000, 2000, 1000, 500, 250, 125, and 62.5 µg/ml. Subsequently, 100 µl of diluted bacterial suspension equivalent to a 0.5 McFarland standard was added to each well. The bacteria were incubated at 37 °C for 24 h after being shaken for 30 min. For fungi, the incubation temperature was 27 °C. The minimum concentration at which no turbidity was observed was considered the Minimum Inhibitory Concentration (MIC). To determine the Minimum Bactericidal Concentration (MBC) and Minimum Fungicidal Concentration (MFC), streak cultures were performed on blood agar plates from the wells that showed no turbidity (MIC and higher concentrations). After 24 h of incubation, the lowest concentration of nanoparticles or extract that was able to kill 99.9 % of the microorganisms was recorded as the MBC and MFC.

2.5. Antioxidant activity

The antioxidant properties of green gold nanoparticles (Sample no. 9) and *tangerine* peel extract were assessed using the 2,2-Diphenyl-1-Picrylhydrazyl (DPPH) radical scavenging assay with Zantax kits. This assay relies on the reduction of the purple DPPH radical to a yellow color by antioxidants, with the extent of color change reflecting the antioxidant efficacy. For this evaluation, 10 µl of different concentrations of sample no. 9 (15.6, 31.2, 62.5, 125, and 250 µg/ml) and *TPE* extract (1.56, 3.12, 6.25, 12.5, and 25 mg/ml) were added to each well, followed by the addition of 250 µl of DPPH solution. The mixture was then shaken for 30 s and allowed to incubate for 20 min. Absorbance was measured at 517 nm. The antioxidant activity of the samples was calculated using the following formula: Scavenging rate (%) $= (1 - A_s/A_0) \times 100$; where, A_s represents the absorbance of the sample, while A_0 represents the absorbance of the blank.

2.6. Photocatalyst performance

The photocatalytic activity of gold nanoparticles synthesized using *tangerine* peel extract (sample no. 9) was investigated under UV and visible light conditions. The pollutants used in this study were rhodamine B as a cationic pollutant and methyl orange as an anionic pollutant. A specified amount of each dye (4 ppm) was diluted in distilled water and poured into a beaker. The experiment was completed by adding 45 mg of the gold photocatalyst to a glass reactor. Prior to irradiation, the mixture was aerated in the dark for 30 min to achieve adsorption-desorption equilibrium. After irradiation, samples were taken from the solution in the beaker at various

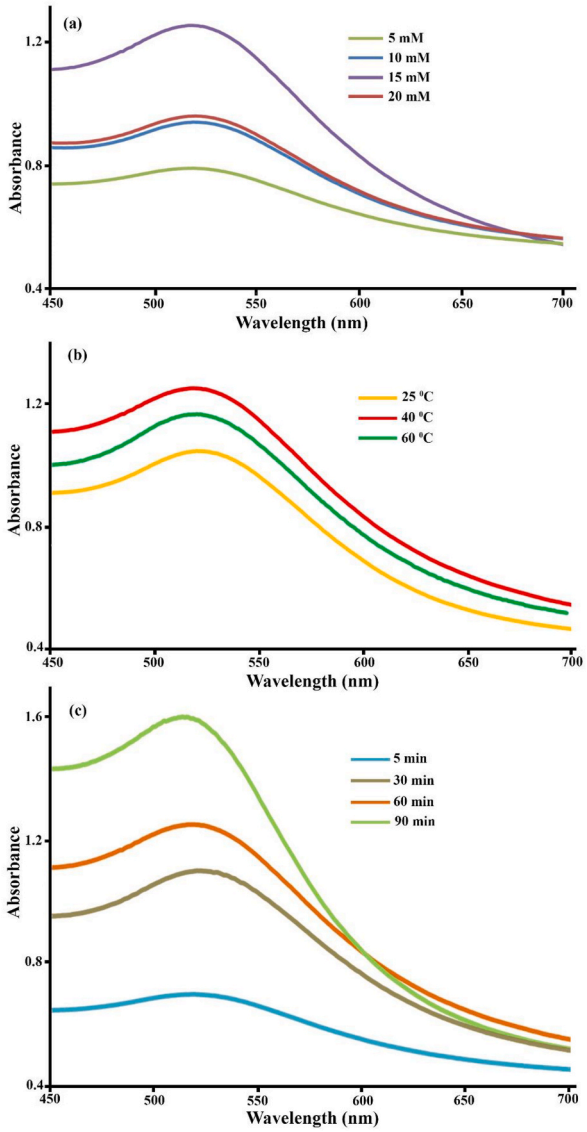

Fig. 1. UV–Vis spectra of the green synthesized gold nanoparticles for optimization at (a) various concentration, temperature (b), and (c) reaction time.

intervals. The absorbance of the solution was measured using a UV–Vis spectrophotometer. Finally, the percentage of pollutant degradation was calculated using the following formula:

Degradation (%) = $[(A_0\text{-}A_t)/A_t]*100$, where A_0 and A_t are related to initial adsorption and adsorption at time t, respectively.

3. Results and discussion

3.1. Spectroscopic analysis (UV–Vis)

Previous research has indicated that achieving optimal reaction conditions can significantly impact the morphology and size of synthesized nanoparticles [36]. Therefore, to determine the optimal reaction conditions, parameters such as temperature (25, 40, and 60 °C), concentration (5, 10, 15, and 20 mM), and reaction time (5, 30, 60, and 90 min) were examined. It is noteworthy that in all experiments, the volume of the *TPE* extract was kept constant at 10 ml. UV–Vis spectroscopy was employed to evaluate the reaction conditions (NanoDrop, BioTek model Epoch). The formation of gold nanoparticles can be identified by a color change from pale yellow to deep red, which leads to the appearance of a Surface Plasmon Resonance (SPR) absorption peak. By analyzing the UV–Vis spectra, the optimal conditions were determined to be at a wavelength of approximately 520 nm. Table 1 summarizes the various conditions for gold nanoparticle synthesis.

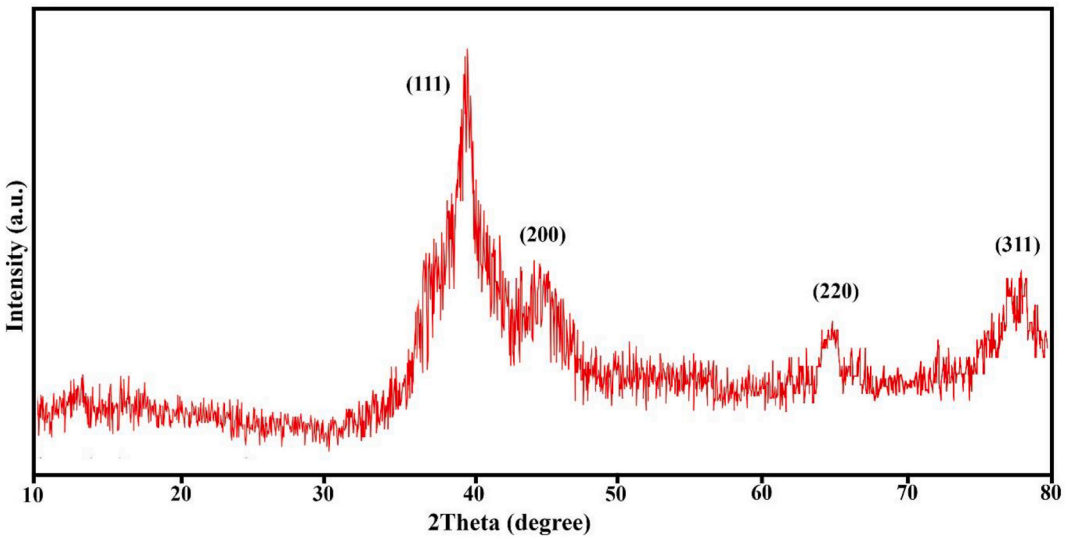

Fig. 2. XRD pattern of Au@*TPE* NPs at optimum conditions: 15 mM of gold concentration, 40 °*C*, and 90 min.

3.1.1. Effect of gold salt concentration on gold nanoparticles

Gold salt concentration is a critical factor in the synthesis of gold nanoparticles. The UV–Vis results regarding the effect of gold salt concentration are illustrated in Fig. 1a. As shown, increasing the gold salt concentration from 5 to 15 mM led to an increase in absorbance, indicating a higher concentration of gold nanoparticles in the solution. However, when the concentration was further increased from 15 to 20 mM, the absorbance decreased. This reduction could be attributed to the aggregation of nanoparticles and the formation of larger-sized products. Therefore, a concentration of 15 mM was determined to be optimal for synthesizing gold nanoparticles using *tangerine* peel extract.

3.1.2. Effect of temperature on gold nanoparticle formation

Temperature is a crucial parameter in the formation of nanoparticles, as excessive temperature can lead to nanoparticle aggregation. Therefore, identifying the optimal temperature is essential. In this study, the reaction was conducted at various temperatures. According to the results shown in Fig. 1b, increasing the reaction temperature from 25 to 40 °*C* led to an increase in UV–Vis peak intensity. This increase was accompanied by a slight blue shift in the wavelength. This trend indicates the formation of nanoparticles with a smaller size and higher quantity. However, when the temperature was increased from 40 to 60 °C, the peak intensity decreased due to nanoparticle aggregation. Thus, 40 °C was determined to be the optimal temperature for the reaction.

3.1.3. Effect of reaction time on gold nanoparticle formation

The results concerning the effect of reaction time on gold nanoparticle synthesis are shown in Fig. 1c. The data indicate that increasing the reaction time from 5 to 90 min resulted in an increased intensity of UV–Vis peaks, reflecting a higher number of nanoparticles in the solution. Consequently, 90 min was selected as the optimal reaction time. In summary, the most efficient conditions for synthesizing gold nanoparticles using *tangerine* peel extract were found to be a concentration of 15 mM, a temperature of 40 °C, and a reaction time of 90 min. These optimized conditions were used for further reactions with the obtained nanoparticles.

3.2. XRD pattern

To examine the crystalline phase and purity of the synthesized nanoparticles, X-ray diffraction (XRD) analysis was conducted. The XRD pattern of Au@*TPE* NPs (sample no 9) is displayed in Fig. 2. As illustrated, the peaks observed at 38.07°, 44.28°, 64.32°, and 77.26° correspond to the crystal planes (111), (200), (220), and (311), respectively. These results are consistent with the standard diffraction pattern for gold nanoparticles (JCPDS card no.04-0784), confirming the presence of well-defined crystalline structures. The size of the synthesized nanoparticles was estimated using the Debye-Scherrer formula [37], which yielded an average particle size of approximately 28 nm. This result is indicative of the nanoparticles uniformity and crystalline quality. In comparison, Shirzadi-Ahodashti et al. [35] synthesized gold nanoparticles using *Pistacia vera* extract, and their XRD analysis revealed four characteristic peaks at 38.2°, 44.22°, 64.79°, and 77.67°. These peaks corresponded to the same crystal planes observed in our study, further validating the accuracy and reliability of our XRD results. The consistency between our results and those reported in the literature suggests that the nanoparticles synthesized using *tangerine* peel extract exhibit similar crystallographic characteristics to those produced with other plant extracts.

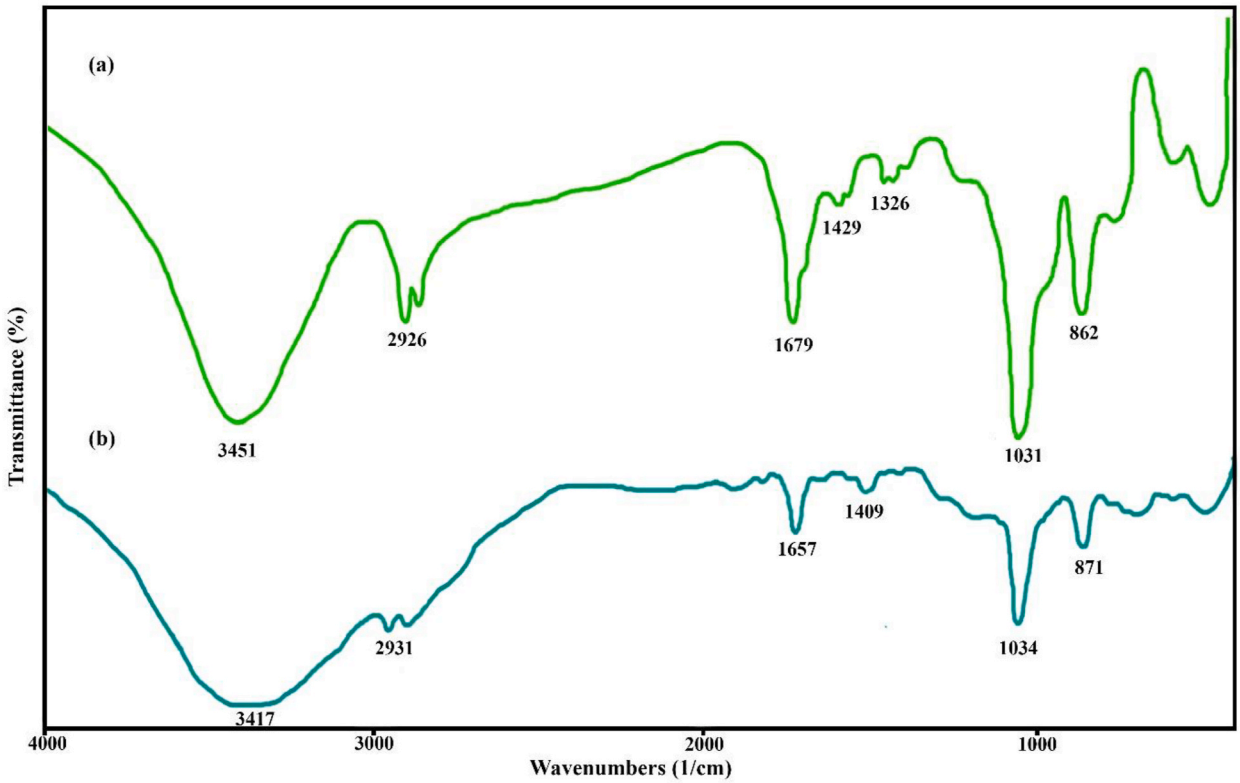

Fig. 3. FT-IR spectra of (a) *tangerine* peel extract and (b) Au@*TPE* NPs at optimum conditions: 15 mM of gold concentration, 40 °*C*, and 90 min.

3.3. FT-IR spectra

To investigate the functional groups, present in *tangerine* peel extract and the gold nanoparticles synthesized using this extract (sample no. 9), fourier transform infrared spectroscopy (FTIR) was employed. The FTIR spectra of the gold nanoparticles and the extract are shown in Fig. 3. As depicted in Fig. 3a, a broad peak around 3451 cm^{-1} is attributed to the stretching vibrations of hydroxyl groups from alcohols or phenols [38]. A weak peak around 2926 cm^{-1} corresponds to C-H stretching vibrations. An absorption peak related to the carbonyl group appeared around 1679 cm^{-1}. Additionally, the peak observed at 1326 cm^{-1} correspond to stretching of the aromatic ring (-C = C) [39]. As previous studies have shown, gold nanoparticles themselves do not exhibit distinctive FTIR spectra [40]. Since the extract interacts with the surface of the gold nanoparticles, the FTIR spectrum reflects this interaction through a decrease in peak intensities and slight shifts. This shift and reduction in peak intensities are illustrated in Fig. 3b. In a study by Shirzadi-Ahodashti et al., where gold nanoparticles were synthesized using *Vicia faba* extract, the FTIR spectrum of the nanoparticles showed no significant difference compared to the extract used [40]. Therefore, our results indicate that the *tangerine* peel extract is indeed present on the surface of the gold nanoparticles.

3.4. EDAX, FESEM, and TEM techniques

The elemental composition of the synthesized nanoparticles was determined using Energy Dispersive X-ray Spectroscopy (EDAX). The EDAX spectra of the Au@*TPE* NPs (sample no. 9) are shown in Fig. 4a. As depicted, the presence of gold, carbon, and oxygen elements is clearly identified. A sharp peak at around 2.2 keV indicates a high percentage of gold in the composition. The presence of oxygen and carbon can be attributed to the components of the extract that are adsorbed onto the gold nanoparticles. In a study by Arunachalam et al. where gold nanoparticles were synthesized using *Memecylon umbellatum* extract, the EDAX spectra also revealed the presence of oxygen and carbon [41]. To examine the surface morphology and approximate size of the Au@*TPE* NPs (sample no. 9), field-emission scanning electron microscopy (FESEM) was employed. The FESEM results, at magnification of 500 nm, are shown in Fig. 4b. The images reveal a spherical morphology and relatively uniform particle sizes, with nanoparticles ranging from approximately 20 to 50 nm. For a more detailed examination of the morphology and precise size of the Au@*TPE* NPs (sample no. 9), Transmission Electron Microscopy (TEM) was used (Fig. 5). The TEM images demonstrate a uniform morphology with particle sizes ranging from 26 ± 5 nm and well-ordered structures. Overall, the combination of EDAX, FESEM, and TEM analyses confirmed that gold nanoparticles were successfully synthesized using a simple and cost-effective method with *tangerine* peel extract. These nanoparticles have shown promise for use in biological and catalytic applications in subsequent studies.

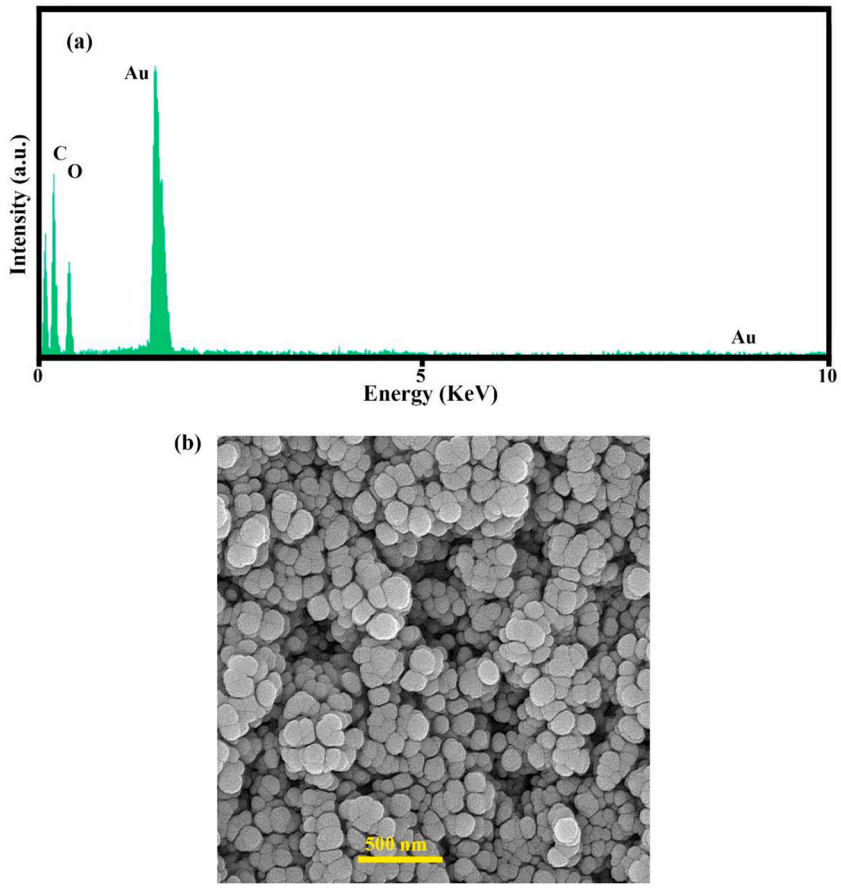

Fig. 4. (a) EDAX and (b) FESEM analysis of Au@*TPE* NPs at optimum conditions: 15 mM of gold concentration, 40 °*C*, and 90 min.

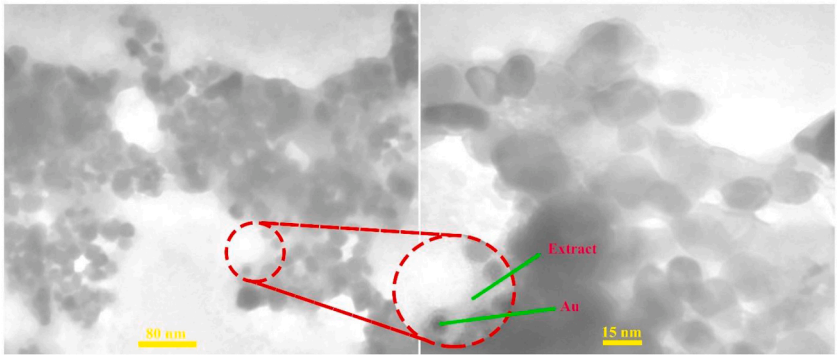

Fig. 5. TEM images of Au@*TPE* NPs at optimum conditions: 15 mM of gold concentration, 40 °*C*, and 90 min.

3.5. Antibacterial and antifungal activities

This study investigated the antibacterial and antifungal activities of gold nanoparticles (sample no. 9) and *tangerine* peel extract against both Gram-negative and Gram-positive bacteria, as well as the fungus *Candida albicans*. The results related to antibacterial and antifungal activities are presented in Tables 2 and 3, respectively. The results demonstrate that the synthesized gold nanoparticles had a significant effect on all tested strains, with varying degrees of effectiveness. As shown in Table 2, the Minimum Inhibitory Concentration (MIC) against *Streptococcus mutans*, *Klebsiella pneumoniae*, *Streptococcus salivarius*, *Pseudomonas aeruginosa*, *Escherichia coli*, and *Staphylococcus aureus* were 125, 31.25, 250, 62.5, 31.25, and 125 μg/ml, respectively. The most significant effects were observed against *Klebsiella pneumoniae*, *Pseudomonas aeruginosa*, and *Escherichia coli*, while the least effect was against *Streptococcus mutans*,

Table 2
MIC and MBC values of *tangerine* peel extract and Au@*TPE* NPs (sample no. 9).

Strain	Au@*TPE* NPs		Extract	
	MIC (μg/ml)	MBC (μg/ml)	MIC (μg/ml)	MBC (μg/ml)
Streptococcus mutans	125	500	>4000	>4000
Klebsiella pneumoniae	31.25	62.5	>4000	>4000
Streptococcus salivarius	250	500	>4000	>4000
Pseudomonas aeruginosa	62.5	125	>4000	>4000
Escherichia coli	31.25	125	>4000	>4000
Staphylococcus aureus	125	125	>4000	>4000

Table 3
MIC and MFC values of *tangerine* peel extract and Au@*TPE* NPs (sample no. 9).

Microorganism	Au@*TPE* NPs		Extract	
	MIC (μg/ml)	MFC (μg/ml)	MIC (μg/ml)	MFC (μg/ml)
Candida Albicans	15.62	62.5	>4000	>4000

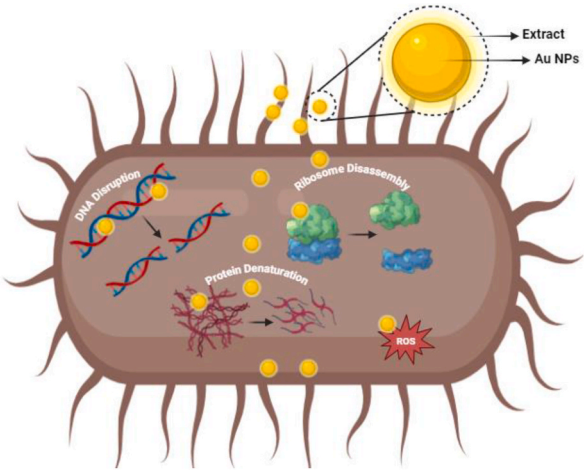

Fig. 6. Proposed mechanism of antibacterial activity of Au@*TPE* NPs.

Streptococcus salivarius, and *Staphylococcus aureus*. Overall, the antibacterial activity was higher against Gram-negative strains compared to Gram-positive ones. The impact of nanoparticles on bacterial strains varies and can be attributed to factors such as cell wall structure, microorganism mechanisms, and overall structural properties. The exact mechanism of action of nanoparticles is not fully understood, but it is hypothesized that smaller nanoparticles with a more uniform structure are more likely to adhere to microorganisms, disrupt cell walls, and cause cell death. This proposed mechanism is illustrated in Fig. 6. According to Morones et al. [42], nanoparticles penetrate bacterial and fungal cells, interact with sulfur and phosphorus-containing compounds like DNA, and ultimately kill microorganisms. Additionally, the MIC values for the antifungal activity of the synthesized gold nanoparticles, as shown in Table 3, indicate that these nanoparticles exhibit very effective antifungal activity, with an MIC of 15.62 μg/ml. Comparing MIC, MBC (Minimum Bactericidal Concentration), and MFC (Minimum Fungicidal Concentration) across various strains and *Candida albicans* showed that the gold nanoparticles synthesized with *tangerine* peel extract have a notable antimicrobial effect compared to the extract alone. Therefore, these results highlight the introduction of a compound with unique antimicrobial properties.

3.6. Antioxidant activity

When the production of free radicals exceeds the capacity of antioxidants to neutralize them, oxidative stress occurs, which can be detrimental to vital molecules in the body, such as nucleic acids. Numerous studies have shown that nanoparticles, such as silver and gold, as well as plant extracts, possess high antioxidant activity [43,44]. Various methods are available to assess this activity. One commonly used method for evaluating antioxidant activity is the DPPH assay. In this method, DPPH is reduced by accepting a hydrogen atom from hydroxyl groups, resulting in a color change of the solution from purple to yellow. In this study, the percentage of DPPH inhibition was investigated using gold nanoparticles and *tangerine* peel extract, with results shown in Fig. 7. As can be seen, the percentage of DPPH inhibition increases with increasing concentration. Specifically, for *tangerine* peel extract Fig. 7a, when the

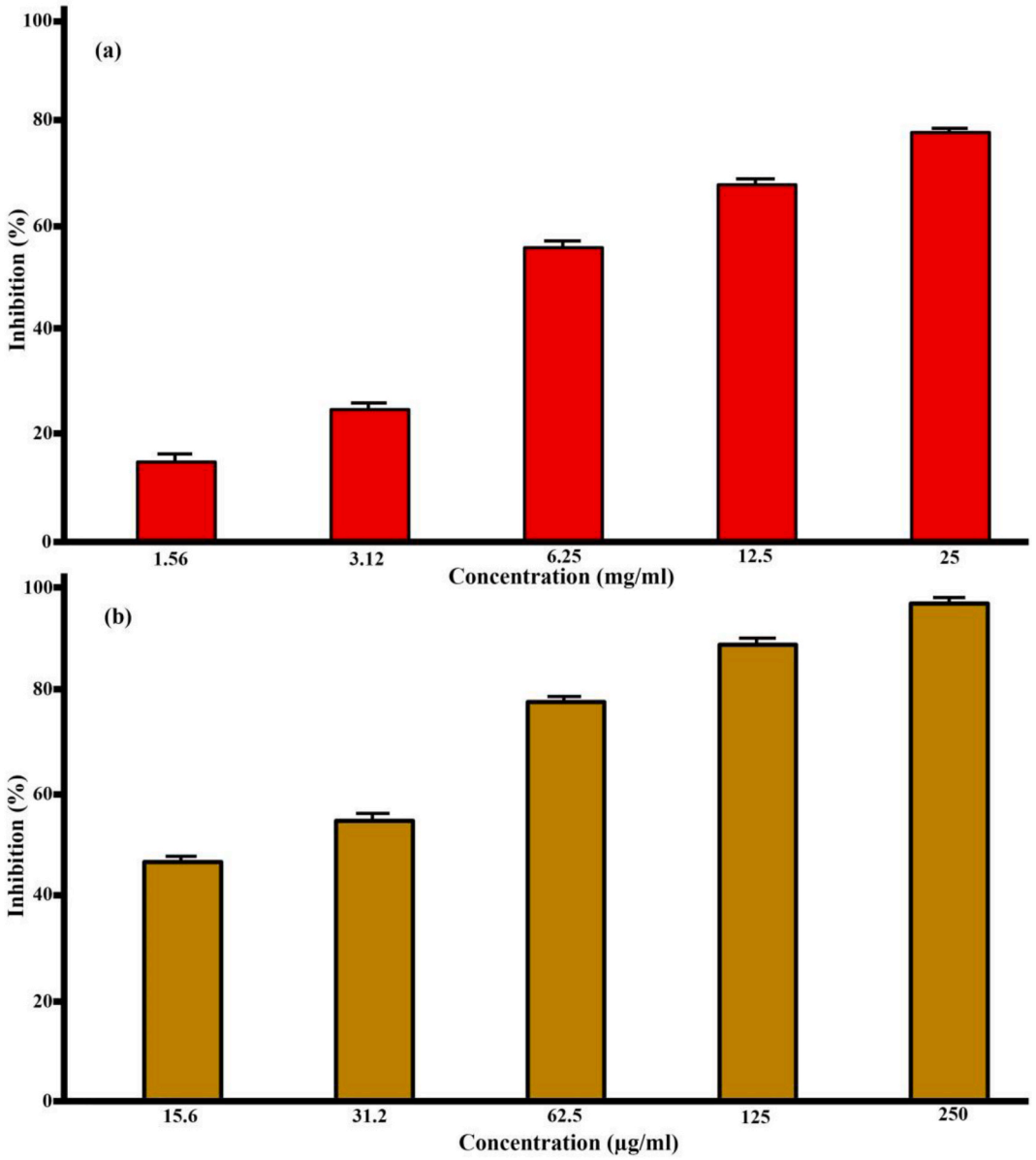

Fig. 7. DPPH inhibition percentage at different concentrations of (a) *tangerine* peel extract and (b) Au@*TPE* NPs at optimum conditions: 15 mM of gold concentration, 40 °*C*, and 90 min.

concentration increased from 1.56 to 25 mg/ml, the percentage of DPPH inhibition increased from 16.7 % to 81.6 %. For gold nanoparticles, increasing the concentration from 15.6 to 250 µg/ml resulted in an increase in the percentage of DPPH inhibition from 45.08 % to 92.7 % (Fig. 7b). Therefore, our results indicate that the gold nanoparticles synthesized with *tangerine* peel extract significantly enhanced antioxidant activity compared to the extract alone. These results are consistent with the findings of Veena et al. [45], who investigated the antioxidant activity of gold nanoparticles synthesized with *Vitex negundo* extract. Their results demonstrated that the percentage of DPPH inhibition increased from 22.15 to 84.67 % with increasing concentration from 20 to 120 µg/ml, which was significantly better than the extract alone.

3.7. Photocatalytic performance

The photocatalytic activity of gold nanoparticles synthesized using *tangerine* peel extract for the degradation of the anionic pollutant methyl orange and the cationic pollutant rhodamine B was investigated under UV and visible light conditions. The results of the degradation of rhodamine B and methyl orange pollutants are illustrated in Figs. 8 and 9. The degradation results for rhodamine B (Fig. 8) indicate that this pollutant was degraded by 93.2 % under UV light and by 74.1 % under visible light. Additionally, Fig. 9 shows

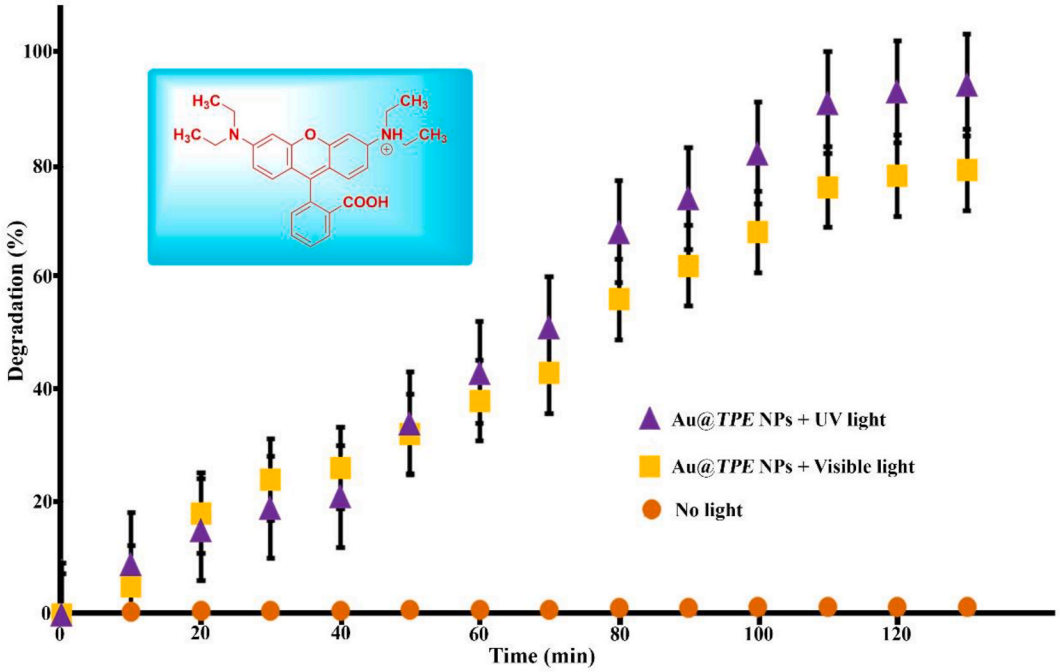

Fig. 8. Rhodamine b degradation under UV and visible light irradiations using Au@*TPE* NPs (sample no. 9).

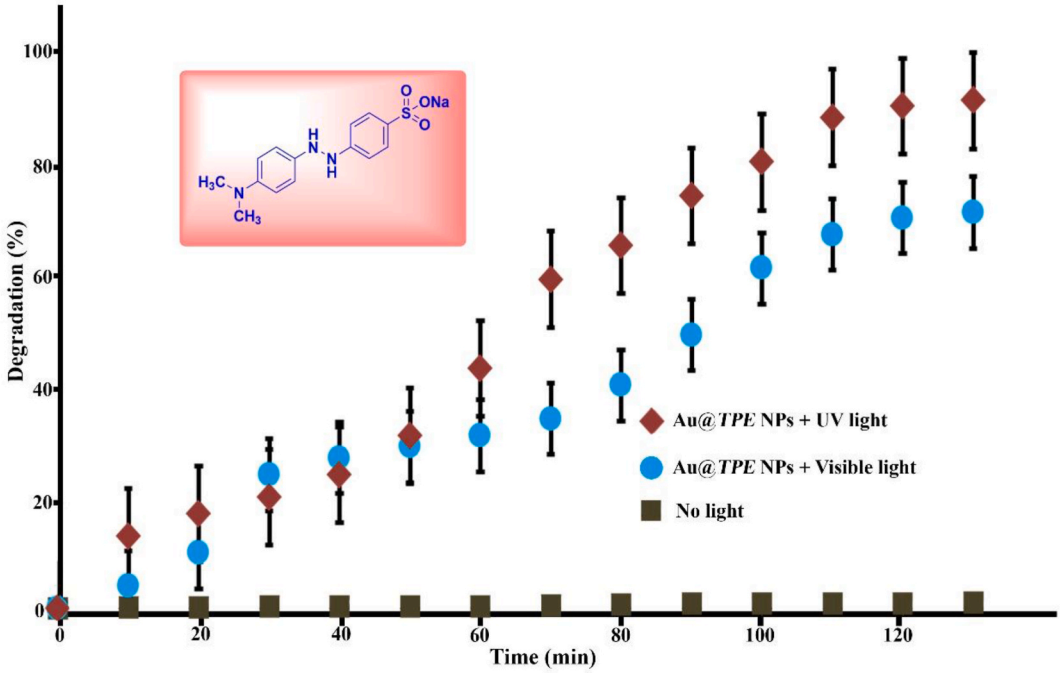

Fig. 9. Methyl orange degradation under UV and visible light irradiations using Au@*TPE* NPs (sample no. 9).

that the anionic pollutant methyl orange was degraded by 88.6 % under UV light and by 67.3 % under visible light. Our results demonstrate the high photocatalytic capability of these nanoparticles. In 2020, Shaikh et al. reported that green silver nanoparticles synthesized with *Shorea robusta* leaf extract degraded 90.41 % of rhodamine B [46]. Therefore, a comparison of our results with those reported by others indicates that gold nanoparticles synthesized using *tangerine* peel extract exhibit excellent photocatalytic performance. A more detailed examination of the results revealed that the degradation percentage of the cationic dye is higher than that of

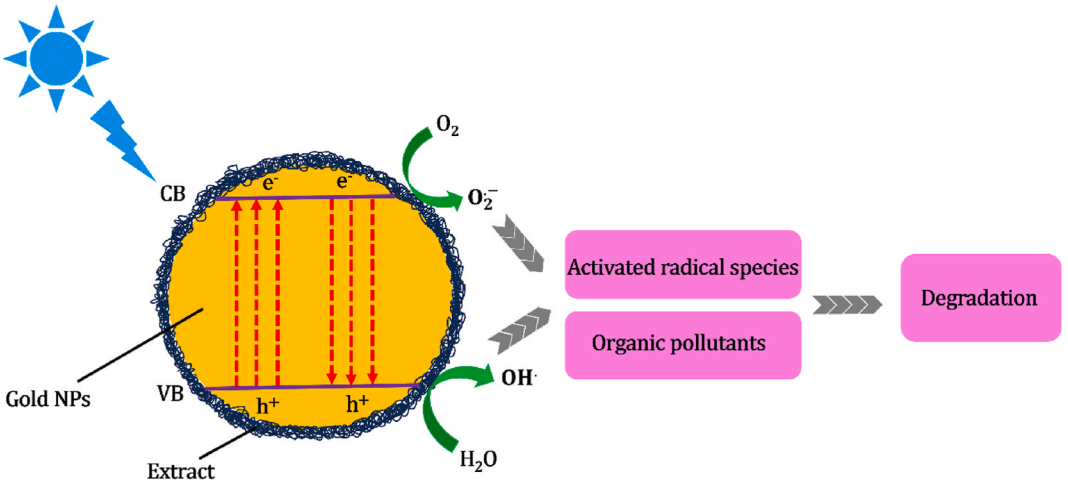

Fig. 10. Decomposition mechanism of organic dyes with Au@*TPE* NPs.

the anionic dye. The presence of positive charges and oxygen-containing groups may be one of the main reasons for this increase. The proposed mechanism for the degradation of pollutants using gold nanoparticles is as follows (Fig. 10):

$$\text{Au@}TPE\text{ NPs} + h\upsilon \rightarrow \text{Au@}TPE\text{ NPs}\left(e^{-}_{CB} + h^{+}_{VB}\right)$$

$$h^{+}_{VB} + H_2O \rightarrow OH^{\cdot} + H^{+}$$

$$e^{-}_{CB} + O_2 \rightarrow O_2^{\cdot -}$$

$$O_2^{\cdot -} + H^{+} \rightarrow H_2O^{\cdot}$$

$$\text{Dye} + OH^{\cdot} \rightarrow \text{Degradation}$$

4. Conclusion

This study demonstrates the successful synthesis of gold nanoparticles using *tangerine* peel extract, offering an eco-friendly and cost-effective alternative to traditional chemical methods. Optimized synthesis conditions produced nanoparticles with an average size of 26 ±5 nm and a spherical morphology. The Au@*TPE* NPs exhibited strong antibacterial and antifungal activities, significant antioxidant properties, and effective photocatalytic degradation of pollutants under UV and sunlight. These promising results suggest that Au@*TPE* NPs have substantial potential for diverse applications in environmental and biomedical fields.

CRediT authorship contribution statement

Seyedeh Masoumeh Ghoreishi: Writing – original draft, Visualization, Validation, Methodology, Investigation, Conceptualization. **Sobhan Mortazavi-Derazkola:** Writing – review & editing, Visualization, Validation, Supervision, Project administration, Formal analysis, Conceptualization.

Declaration of Competing Interest

The authors declare that they have no known competing financial interests or personal relationships that could have appeared to influence the work reported in this paper.

Acknowledgment

This research is the result of research with ethical code IR. BUMS.REC.1398.346. We are grateful to Birjand University of Medical Sciences for supporting this research.

References

[1] M.A. Ebrahimzadeh, Z. Hashemi, M. Mohammadyan, M. Fakhar, S. Mortazavi-Derazkola, In vitro cytotoxicity against human cancer cell lines (MCF-7 and AGS), antileishmanial and antibacterial activities of green synthesized silver nanoparticles using Scrophularia striata extract, Surface. Interfac. 23 (2021) 100963.

[2] Z. Hashemi, M.A. Ebrahimzadeh, P. Biparva, S. Mortazavi-Derazkola, H.R. Goli, F. Sadeghian, M. Kardan, A. Rafiei, Biogenic silver and zero-valent iron nanoparticles by feijoa: biosynthesis, characterization, cytotoxic, antibacterial and antioxidant activities, Anti Cancer Agents Med. Chem. 20 (2020) 1673–1687.
[3] S.K. Saxena, R. Nyodu, S. Kumar, V.K. Maurya, Current advances in nanotechnology and medicine, in: S.K. Saxena, S.M.P. Khurana (Eds.), NanoBioMedicine, Springer Singapore, Singapore, 2020, pp. 3–16.
[4] T. Patil, V. Khot, A. Pandey-Tiwari, Single-step antibiotic-mediated synthesis of kanamycin-conjugated gold nanoparticles for broad-spectrum antibacterial applications, Lett. Appl. Microbiol. 75 (2022) 913–923.
[5] S. Mortazavi-Derazkola, M. Reza Naimi-Jamal, S. Masoumeh Ghoreishi, Synthesis, characterization, and atenolol delivery application of functionalized mesoporous hydroxyapatite nanoparticles prepared by microwave-assisted Co-precipitation method, Curr. Drug Deliv. 13 (2016) 1123–1129.
[6] V. Goranov, Biomaterials functionalized with magnetic nanoparticles for tissue engineering: between advantages and challenges, Biomaterials and Biosystems 15 (2024) 100100.
[7] H. Liu, S. Wang, R. Zhuo, Y. Duan, J. Wang, Y. Li, J. Yang, Size-controlled synthesis of copper oxide nanoparticles with a supercritical hydrothermal synthesis method, Powder Technol. 444 (2024) 119803.
[8] L. Seravalli, M. Bosi, P. Fiorenza, S.E. Panasci, D. Orsi, E. Rotunno, L. Cristofolini, F. Rossi, F. Giannazzo, F. Fabbri, Gold nanoparticle assisted synthesis of MoS2 monolayers by chemical vapor deposition††Electronic supplementary information (ESI) available. See, Nanoscale Adv. 3 (2021) 4826–4833, https://doi.org/10.1039/d1na00367d.
[9] N.A. Salleh, A.H. Mohammad, Z. Zakaria, B. Deghfel, M.K. Yaakob, W. Rahiman, S. Kheawhom, A.A. Mohamad, Microwave assisted synthesis of nickel oxide nanoparticles at different pH via sol gel method: experimental and first-principles investigations, Inorg. Chem. Commun. 164 (2024) 112415.
[10] O.V. Kharissova, B.I. Kharisov, C.M. Oliva González, Y.P. Méndez, I. López, Greener synthesis of chemical compounds and materials, R. Soc. Open Sci. 6 (2019) 191378.
[11] G. Kasi, S. Thanakkasaranee, P. Seesuriyachan, P. Rachtanapun, One–pot synthesis of gold nanoparticles using Pandanus amaryllifolius leaf extract and their antibacterial, antioxidant, anticancer, and ecotoxicity assessment, Biocatal. Agric. Biotechnol. 50 (2023) 102695.
[12] R. Shegokar, M. Nakach, Chapter 4 - large-scale manufacturing of nanoparticles—an industrial outlook, in: R. Shegokar (Ed.) Drug Delivery Aspects, Elsevier2020, pp. 57-77.
[13] T. Khan, N. Ullah, M.A. Khan, Z.-u.-R. Mashwani, A. Nadhman, Plant-based gold nanoparticles; a comprehensive review of the decade-long research on synthesis, mechanistic aspects and diverse applications, Adv. Colloid Interface Sci. 272 (2019) 102017.
[14] V.S. Parkhe, T.P. Patil, A.P. Tiwari, Biowaste-mediated green synthesis of gold nanoparticles using Solanum tuberosum peel extract for antibacterial, antioxidant, and photocatalytic applications, Nanotechnology for Environmental Engineering 8 (2023) 1067–1081.
[15] T.P. Patil, A.A. Vibhute, S.L. Patil, T.D. Dongale, A.P. Tiwari, Green synthesis of gold nanoparticles via Capsicum annum fruit extract: characterization, antiangiogenic, antioxidant and anti-inflammatory activities, Applied Surface Science Advances 13 (2023) 100372.
[16] A. Fouda, A.M. Eid, E. Guibal, M.F. Hamza, S.E.-D. Hassan, D.H.M. Alkhalifah, D. El-Hossary, Green synthesis of gold nanoparticles by aqueous extract of zingiber officinale: characterization and insight into antimicrobial, antioxidant, and in vitro cytotoxic activities, Appl. Sci. 12 (2022) 12879.
[17] K.S. Alshallash, A.M. Eid, S.E.-D. Hassan, M.A. Abdel-Rahman, A.S. Alawam, M.F. Hamza, A. Fouda, Zingiber officinale-Mediated biosynthesis of bimetallic Gold/Silver (BAu/Ag) nanoalloys; an insight into antiviral and anticancer activities, J. King Saud Univ. Sci. 36 (2024) 103243.
[18] Z. Samadi, K. Yaghmaeian, S. Mortazavi-Derazkola, R. Khosravi, R. Nabizadeh, M. Alimohammadi, Facile green synthesis of zero-valent iron nanoparticles using barberry leaf extract (GnZVI@BLE) for photocatalytic reduction of hexavalent chromium, Bioorg. Chem. 114 (2021) 105051.
[19] A. Naghizadeh, S. Mohammadi-Aghdam, S. Mortazavi-Derazkola, Novel CoFe2O4@ZnO-CeO2 ternary nanocomposite: sonochemical green synthesis using Crataegus microphylla extract, characterization and their application in catalytic and antibacterial activities, Bioorg. Chem. 103 (2020) 104194.
[20] S. Stankic, S. Suman, F. Haque, J. Vidic, Pure and multi metal oxide nanoparticles: synthesis, antibacterial and cytotoxic properties, J. Nanobiotechnol. 14 (2016) 73.
[21] A.J. Huh, Y.J. Kwon, "Nanoantibiotics": a new paradigm for treating infectious diseases using nanomaterials in the antibiotics resistant era, J. Contr. Release 156 (2011) 128–145.
[22] J. Ismy, M. Syukri, D.R. Emril, N. Sekarwana, J. Ismy, Superoxide dismutase reduces creatinine and NGAL by restoring oxidative balance during sepsis, Emerging Science Journal 6 (2022) 286–294.
[23] I. Wan Norfazilah Wan, S. Mohamad Irfan Arif Irwan, M. Nur Hanisah Abd, B. Nurul Hidayah Abu, Y. Hartina Mohd, S. Nurlin Abu, Adsorption behavior of heavy metal ions by hybrid inulin-TEOS for water treatment, Civil Engineering Journal (2022) 1787–1798.
[24] A.K. Abdalhussain, H.W. Ahmed, H.Y. Falah, Effect of applying cold plasma on structural, antibacterial and self cleaning properties of α-Fe2O3 (HEMATITE) thin film, Emerging Science Journal (2022) 75–85.
[25] N. Thakur, N. Thakur, A. Kumar, V.K. Thakur, S. Kalia, V. Arya, A. Kumar, S. Kumar, G.Z. Kyzas, A critical review on the recent trends of photocatalytic, antibacterial, antioxidant and nanohybrid applications of anatase and rutile TiO2 nanoparticles, Sci. Total Environ. 914 (2024) 169815.
[26] T. Cherian, D. Maity, R.T. Rajendra Kumar, G. Balasubramani, C. Ragavendran, S. Yalla, R. Mohanraju, W.J.G.M. Peijnenburg, Green chemistry based gold nanoparticles synthesis using the marine bacterium lysinibacillus odysseyi PBCW2 and their multitudinous activities, Nanomaterials 12 (2022) 2940.
[27] X. Gu, Z. Xu, L. Gu, H. Xu, F. Han, B. Chen, X. Pan, Preparation and antibacterial properties of gold nanoparticles: a review, Environ. Chem. Lett. 19 (2021) 167–187.
[28] S. Medici, M. Peana, D. Coradduzza, M.A. Zoroddu, Gold nanoparticles and cancer: detection, diagnosis and therapy, Semin. Cancer Biol. 76 (2021) 27–37.
[29] B. Ahmad, N. Hafeez, S. Bashir, A. Rauf, R. Mujeeb ur, Phytofabricated gold nanoparticles and their biomedical applications, Biomed. Pharmacother. 89 (2017) 414–425.
[30] X. Hu, Y. Zhang, T. Ding, J. Liu, H. Zhao, Multifunctional gold nanoparticles: a novel nanomaterial for various medical applications and biological activities, Front. Bioeng. Biotechnol. 8 (2020).
[31] J. Gubitosa, V. Rizzi, P. Fini, A. Laurenzana, G. Fibbi, C. Veiga-Villauriz, F. Fanelli, F. Fracassi, A. Onzo, G. Bianco, C. Gaeta, A. Guerrieri, P. Cosma, Biomolecules from snail mucus (Helix aspersa) conjugated gold nanoparticles, exhibiting potential wound healing and anti-inflammatory activity, Soft Matter 16 (2020) 10876–10888.
[32] D. Susanna, R.M. Balakrishnan, J. Ponnan Ettiyappan, Ultrasonication-assisted green synthesis and characterization of gold nanoparticles from Nothapodytes foetida: an assessment of their antioxidant, antibacterial, anticancer and wound healing potential, J. Drug Deliv. Sci. Technol. 87 (2023) 104740.
[33] S. Rokkarukala, T. Cherian, C. Ragavendran, R. Mohanraju, C. Kamaraj, Y. Almoshari, A. Albariqi, M.H. Sultan, A. Alsalhi, S. Mohan, One-pot green synthesis of gold nanoparticles using Sarcophyton crassocaule, a marine soft coral: assessing biological potentialities of antibacterial, antioxidant, anti-diabetic and catalytic degradation of toxic organic pollutants, Heliyon 9 (2023) e14668.
[34] S.S.J. Princy, C. Hentry, M.R. Bindhu, R. Rajakrishnan, A. Alfarhan, S. Arokiyaraj, Assessing the anticancer, antibacterial and photocatalytic potency of Solanum nigrum root mediated gold and silver nanoparticles, South Afr. J. Bot. 166 (2024) 38–51.
[35] M. Shirzadi-Ahodashti, Z.M. Mizwari, S. Mohammadi-Aghdam, S. Ahmadi, M. Ali Ebrahimzadeh, S. Mortazavi-Derazkola, Optimization and evaluation of anticancer, antifungal, catalytic, and antibacterial activities: biosynthesis of spherical-shaped gold nanoparticles using Pistacia vera hull extract (AuNPs@PV), Arab. J. Chem. 16 (2023) 104423.
[36] M. Shirzadi-Ahodashti, Z. Hashemi, Y. Mortazavi, K. Khormali, S. Mortazavi-Derazkola, M.A. Ebrahimzadeh, Discovery of high antibacterial and catalytic activities against multi-drug resistant clinical bacteria and hazardous pollutants by biosynthesized of silver nanoparticles using Stachys inflata extract (AgNPs@SI), Colloids Surf. A Physicochem. Eng. Asp. 617 (2021) 126383.
[37] M. Zare-Bidaki, A. Ghasempour, P. Mohammadparast-Tabas, S.M. Ghoreishi, E. Alamzadeh, R. Javanshir, B.N. Le, M. Barakchi, M. Fattahi, S. Mortazavi-Derazkola, Enhanced in vivo wound healing efficacy and excellent antibacterial, antifungal, antioxidant and anticancer activities via AgNPs@PCS, Arab. J. Chem. 16 (2023) 105194.

[38] F. Barzegarparaay, H. Najafzadehvarzi, R. Pourbagher, H. Parsian, S.M. Ghoreishi, S. Mortazavi-Derazkola, Green synthesis of novel selenium nanoparticles using Crataegus monogyna extract (SeNPs@CM) and investigation of its toxicity, antioxidant capacity, and anticancer activity against MCF-7 as a breast cancer cell line, Biomass Convers. Biorefinery 14 (2024) 25369–25378.
[39] Z. Kiani, H. Aramjoo, E. Chamani, M. Siami-Aliabad, S. Mortazavi-Derazkola, In vitro cytotoxicity against K562 tumor cell line, antibacterial, antioxidant, antifungal and catalytic activities of biosynthesized silver nanoparticles using Sophora pachycarpa extract, Arab. J. Chem. 15 (2022) 103677.
[40] M. Shirzadi-Ahodashti, Z.M. Mizwari, B. Jafarkhani, S. mohamadzadeh, M. Abbastabar, F. Motafeghi, F. Sadeghi Lalerdi, M. Ali Ebrahimzadeh, S. Mortazavi-Derazkola, Biogenic synthesis of spherical-shaped noble metal nanoparticles using Vicia faba extract (X@VF, X = Au, Ag) for photocatalytic degradation of organic hazardous dye and their in vitro antifungal, antibacterial and anticancer activities, Inorg. Chem. Commun. 146 (2022) 110042.
[41] K.D. Arunachalam, S.K. Annamalai, S. Hari, One-step green synthesis and characterization of leaf extract-mediated biocompatible silver and gold nanoparticles from Memecylon umbellatum, Int J Nanomedicine 8 (2013) 1307–1315.
[42] J.R. Morones, J.L. Elechiguerra, A. Camacho, K. Holt, J.B. Kouri, J.T. Ramírez, M.J. Yacaman, The bactericidal effect of silver nanoparticles, Nanotechnology 16 (2005) 2346.
[43] V. Sekar, M.M. Al-Ansari, J. Narenkumar, L. Al-Humaid, P. Arunkumar, A. Santhanam, Synthesis of gold nanoparticles (AuNPs) with improved anti-diabetic, antioxidant and anti-microbial activity from Physalis minima, J. King Saud Univ. Sci. 34 (2022) 102197.
[44] A. Aji, D. Oktafiani, A. Yuniarto, A.K. Amin, Biosynthesis of gold nanoparticles using Kapok (Ceiba pentandra) leaf aqueous extract and investigating their antioxidant activity, J. Mol. Struct. 1270 (2022) 133906.
[45] S. Veena, T. Devasena, S.S.M. Sathak, M. Yasasve, L.A. Vishal, Green synthesis of gold nanoparticles from Vitex negundo leaf extract: characterization and in vitro evaluation of antioxidant–antibacterial activity, J. Cluster Sci. 30 (2019) 1591–1597.
[46] W.A. Shaikh, S. Chakraborty, R.U. Islam, Photocatalytic degradation of rhodamine B under UV irradiation using Shorea robusta leaf extract-mediated bio-synthesized silver nanoparticles, Int. J. Environ. Sci. Technol. 17 (2020) 2059–2072.